

Titanium, Zirconium, and Hafnium Metal Atom Reactions with CF₄, CCl₄, and CF₂Cl₂: A Matrix Isolation Spectroscopic and DFT Investigation of Triplet XC≡MX₃ Complexes

Jonathan T. Lyon and Lester Andrews*

Department of Chemistry, University of Virginia, P.O. Box 400319, Charlottesville, Virginia 22904-4319

Received February 6, 2007

Laser-ablated group 4 transition metal atoms react with CF₄ to form triplet state electron-deficient FC≡MF₃ methyldyne complexes, which are identified by their infrared spectra and comparison to density functional vibrational frequency calculations of stable possible products. Of particular interest in these complexes are the strong C–X bonds and carbon–metal π bonding. The two unpaired electrons on carbon are drawn to the electron-deficient transition metal center, forming a partially filled triple bond, which is approximately equal in length to a classical C=M double bond. Reactions with carbon tetrachloride form the analogous ClC≡MCl₃ complexes, whereas reactions with CF₂Cl₂ form a mixture of FC≡MFCl₂ and ClC≡MF₂Cl species. The FC≡MFCl₂ complexes involving more α -Cl transfer are favored in the reaction of excited metal atoms during sample deposition, but UV irradiation photoisomerizes FC≡MFCl₂ to the lower energy ClC≡MF₂Cl complexes with more α -F transfer to the metal center.

Introduction

Transition metal compounds are important for their roles in catalysis. In particular, the study of organotitanium compounds has been an active field of research.^{1–3} Recently, nanostructural carbon has been synthesized by the reaction of titanium carbide with chlorine gas, with TiCl₄ as a byproduct of the reaction.^{4–6} Freon compounds are hazardous to the ozone layer, and the activation of C–X bonds is a necessary process in their remediation.⁷ However, C–F bonds are the strongest known carbon single bond,⁸ and their activation is not always trivial.

We have recently reacted group 4 transition metal atoms with CH₃X precursors (X = H, F, Cl, and Br).⁹ In these experiments, the primary reaction products are the double-bonded CH₂=MHX methyldiene complexes, which show considerable agostic interactions between the transition metal center and one set of C–H-bonding electrons. Titanium, zirconium, and hafnium all combined with CH₂X₂ (X = F and Cl) to yield the very stable CH₂=MX₂ methyldienes, which showed no agostic distortions,^{10–12}

but reactions with CHX₃ (X = F and Cl) yielded triplet HC≡MX₃ species (except for Ti + CHF₃, where the reaction stopped at the CHF=TiF₂ intermediate).^{11,12} These complexes are unique in that the two unpaired electrons on carbon are shared partially with the transition metal center. The formation of this novel electron-deficient C≡M triple bond is more prevalent in the FC≡TiF₃ and ClC≡TiCl₃ complexes in the reaction between laser-ablated titanium atoms and CX₄ (X = F and Cl).¹³ We now report on reactions of the entire group 4 transition metal series with CF₄ and CCl₄, and the mixed chlorofluorocarbon CF₂Cl₂ for comparison. A particular question we want to answer in this investigation is whether FC≡MFCl₂, ClC≡MF₂Cl, neither complex, or both complexes are formed and how this distortion of symmetry effects the partially filled C≡M triple bonds.

Experimental and Theoretical Methods

Our experimental design has been described in detail previously.¹⁴ In brief, metal atoms, produced by laser ablation with a Nd:YAG laser, were co-deposited with a dilute mixture (0.25–1.0%) of reagent vapor (CF₄, CCl₄, CF₂Cl₂, ¹³CCl₄, or ¹³CF₂Cl₂)¹⁵ in argon onto a CsI window cooled to 8 K. The resulting reaction products were frozen in the inert matrix, and the infrared spectrum was recorded on a Nicolet Magna 550 spectrometer. Matrix samples were irradiated for 10 min periods by a medium-pressure mercury arc lamp with the globe removed ($\lambda > 220$ nm) with or without a Pyrex ($\lambda > 290$ nm) filter and subsequently annealed to various temperatures. Additional infrared spectra were recorded following each procedure.

* Corresponding author. E-mail: isa@virginia.edu.

(1) Bini, F.; Rosier, C.; Saint-Arroman, R. P.; Neumann, E.; Dadlemont, C.; de Mallmann, A.; Lefebvre, F.; Niccolai, G. P.; Basset, J.-M.; Crocker, M.; Buijink, J.-K. *Organometallics* **2006**, *25*, 3743.

(2) Zhang, Y.; Mu, Y. *Organometallics* **2006**, *25*, 631.

(3) Anthis, J. W.; Filippov, I.; Wigley, D. E. *Inorg. Chem.* **2004**, *43*, 716.

(4) Leis, J.; Perkson, A.; Arulepp, M.; Nigu, P.; Svensson, G. *Carbon* **2002**, *40*, 1559.

(5) Zetterström, P.; Urbonaitė, S.; Lindberg, F.; Delaplane, R. G.; Leis, J.; Svensson, G. *J. Phys.: Condens. Matter* **2005**, *17*, 3509.

(6) Permann, L.; Lätt, M.; Leis, J.; Arulepp, M. *Electrochim. Acta* **2006**, *51*, 1274.

(7) Molina, M. J.; Rowland, F. S. *Nature* **1974**, *249*, 810.

(8) Strauss, S. H. *Chem. Rev.* **1993**, *93*, 927.

(9) Andrews, L.; Cho, H.-G. *Organometallics* **2006**, *25*, 4040, and references therein.

(10) Lyon, J. T.; Andrews, L. *Organometallics* **2006**, *25*, 1341 (Ti + CH₂F₂).

(11) Lyon, J. T.; Andrews, L. *Inorg. Chem.* **2007**, *46*, ASAP 12/19/06 (Ti, Zr, and Hf + CH₂F₂ and CHF₃).

(12) Lyon, J. T.; Andrews, L. *Organometallics* **2007**, *26*, 332 (Ti, Zr, and Hf + CH₂Cl₂ and CHCl₃).

(13) Lyon, J. T.; Andrews, L. *Inorg. Chem.* **2006**, *45*, 9858 (Ti + CF₄ and CCl₄).

(14) (a) Andrews, L. *Chem. Soc. Rev.* **2004**, *33*, 123. (b) Andrews, L.; Citra, A. *Chem. Rev.* **2002**, *102*, 885, and references therein.

(15) (a) Prochaska, F. T.; Andrews, L. *J. Chem. Phys.* **1978**, *68*, 5568. (b) Prochaska, F. T.; Andrews, L. *J. Chem. Phys.* **1978**, *68*, 5577. (c) Milligan, D. E.; Jacox, M. E.; McAuley, J. H.; Smith, C. E. *J. Mol. Spectrosc.* **1973**, *45*, 377.

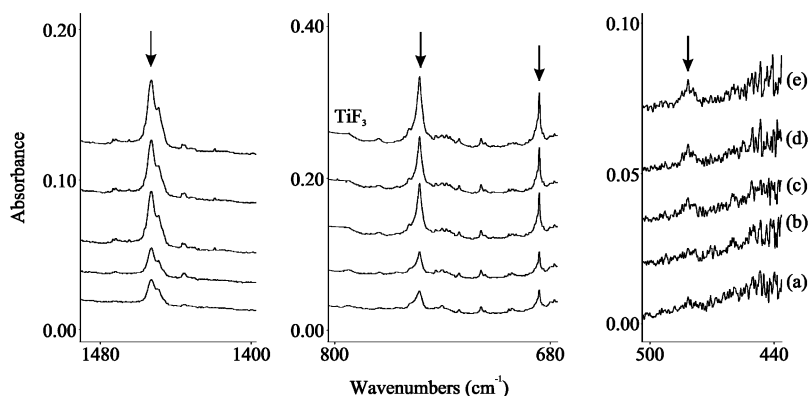


Figure 1. Infrared spectra in the 1480–1400, 800–680, and 500–440 cm^{-1} regions taken after (a) laser-ablated titanium atoms were reacted with 1.0% CF_4/Ar during condensation at 8 K for 1 h, and the resulting matrix was subjected to (b) irradiation with light $\lambda > 290$ nm, (c) irradiation with $\lambda > 220$ nm, (d) annealing to 30 K, and (e) irradiation with $\lambda > 220$ nm. Arrows indicate product absorptions.

Theoretical computations on possible reaction products and intermediates were performed using the Gaussian 98 program.¹⁶ In all instances, the B3LYP hybrid density functional was employed.¹⁷ All atoms were given a moderate 6-311+G(2d) basis set except for the transition metal center, where the SDD pseudopotential was utilized.^{18,19} Such DFT calculations predict vibrational frequencies with reasonable accuracy for transition metal, halogen compounds. For example, the strong t_2 mode for TiF_4 is computed as 805 cm^{-1} , which is slightly higher than the 800 cm^{-1} observed value.²⁰ The strong antisymmetric Ti–Cl stretching frequency for TiCl_4 is calculated at 500 cm^{-1} , which compares to the 503 cm^{-1} argon matrix observation.²¹ All energy values reported include zero-point vibrational corrections. Our electronic energy calculations find TiCl_4 to be 285 kcal/mol lower in energy than the Ti atom and two Cl_2 molecules, and gas phase thermodynamic values give 295 ± 2 kcal/mol.²² Although we cannot determine the absolute accuracy of the new product energies, we believe that the relative stabilities are correct. We employ calculated product energies and vibrational frequencies to help identify the new product molecules in these reactions.

Results and Discussion

Products formed in the reactions of group 4 transition metals with CF_4 , CCl_4 , and CF_2Cl_2 will be reported in turn. Irradiation of these precursors by the laser-ablation plume gave weak metal-independent absorptions for radical and intermediate species that

have been reported by earlier workers.¹⁵ Some of these are labeled in the chlorofluoromethane figures.

Ti + CF_4 and CCl_4 . Titanium reactions with carbon tetrafluoride and carbon tetrachloride have been reported recently.¹³ Here we discuss these assignments to provide a foundation for this article and report computed parameters for these complexes at the same level of theory that will be used for the zirconium and hafnium analogues in order to allow for comparisons and analysis of group trends.

The reaction between titanium and CF_4 produced four absorptions at 481.7 , 686.1 , 752.8 , and 1453.1 cm^{-1} (Figure 1), which increased together on UV irradiation. These product peaks are assigned to the symmetric (FC)–Ti stretching mode, two Ti–F stretching frequencies, and a very high C–F stretching mode, respectively.¹³ The characterization of these functional group vibrations leads to two possible products. Analogous to titanium reactions with CH_4 , CH_3F , CH_2F_2 , and CHF_3 ,^{10,11,23–25} the singlet $\text{CF}_2=\text{TiF}_2$ methyldene complex was considered. However, this possible product is predicted to have strong infrared active modes at 688.8 , 770.5 , 1087.7 , and 1237.9 cm^{-1} . Although the two Ti–F stretching modes are in fairly good agreement with the observed product peaks, the C–F stretching modes are predicted too far below the observed frequency to warrant this assignment. Triplet $\text{FC}\div\text{TiF}_3$ is calculated to be 19 kcal/mol lower in energy than the possible singlet methyldene and 146 kcal/mol below Ti and CF_4 . This very stable product is computed to have a weak band at 480.3 cm^{-1} and strong infrared absorptions at 705.6 , 766.2 , and 1470.2 cm^{-1} , which reproduce the observed vibrations (Table 1) within the accuracy expected for DFT.^{23–26} We must point out the very high-frequency diagnostic C–F stretching mode. Hence, the observed spectrum is assigned to the triplet $\text{FC}\div\text{TiF}_3$ species with a unique very high C–F stretching mode.¹³ In addition, a weak 792.5 cm^{-1} band increased slightly on UV irradiation, which is appropriate for TiF_3 in solid argon.²⁷

Similarly, titanium reactions with carbon tetrachloride produced two product absorptions at 487.0 and 1151.5 cm^{-1} . In

(16) Frisch, M. J.; Trucks, G. W.; Schlegel, H. B.; Scuseria, G. E.; Robb, M. A.; Cheeseman, J. R.; Zakrzewski, V. G.; Montgomery, J. A., Jr.; Stratmann, R. E.; Burant, J. C.; Dapprich, S.; Millam, J. M.; Daniels, A. D.; Kudin, K. N.; Strain, M. C.; Farkas, O.; Tomasi, J.; Barone, V.; Cossi, M.; Cammi, R.; Mennucci, B.; Pomelli, C.; Adamo, C.; Clifford, S.; Ochterski, J.; Petersson, G. A.; Ayala, P. Y.; Cui, Q.; Morokuma, K.; Rega, N.; Salvador, P.; Dannenberg, J. J.; Malick, D. K.; Rabuck, A. D.; Raghavachari, K.; Foresman, J. B.; Cioslowski, J.; Ortiz, J. V.; Baboul, A. G.; Stefanov, B. B.; Liu, G.; Liashenko, A.; Piskorz, P.; Komaromi, I.; Gomperts, R.; Martin, R. L.; Fox, D. J.; Keith, T.; Al-Laham, M. A.; Peng, C. Y.; Nanayakkara, A.; Challacombe, M.; Gill, P. M. W.; Johnson, B.; Chen, W.; Wong, M. W.; Andres, J. L.; Gonzalez, C.; Head-Gordon, M.; Replogle, E. S.; Pople, J. A. *Gaussian 98*, Revision A.11.4; Gaussian, Inc.: Pittsburgh, PA, 2002.

(17) (a) Becke, A. D. *J. Chem. Phys.* **1993**, *98*, 5648. (b) Lee, C.; Yang, Y.; Parr, R. G. *Phys. Rev. B* **1988**, *37*, 785.

(18) Frisch, M. J.; Pople, J. A.; Binkley, J. S. *J. Chem. Phys.* **1984**, *80*, 3265.

(19) Andrae, D.; Haeussermann, U.; Dolg, M.; Stoll, H.; Preuss, H. *Theor. Chim. Acta* **1990**, *77*, 123.

(20) Beattie, I. R.; Jones, P. J. *J. Chem. Phys.* **1989**, *90*, 5209.

(21) Hastie, J. W.; Hauge, R. H.; Margrave, J. L. *High Temp. Sci.* **1971**, *3*, 257.

(22) Cox, J. D.; Wagman, D. D.; Medvedev, V. A. *CODATA Key Values for Thermodynamics*; Hemisphere Publishing Corp.: New York, 1989.

(23) Andrews, L.; Cho, H.-G.; Wang, X. *Inorg. Chem.* **2005**, *44*, 4834 (Ti + CH_4).

(24) Cho, H.-G.; Andrews, L. *Inorg. Chem.* **2004**, *43*, 5253 (Ti + CH_3F).

(25) Cho, H.-G.; Andrews, L. *J. Phys. Chem. A* **2004**, *108*, 6294 (Ti + CH_3F).

(26) (a) Scott, A. P.; Radom, L. *J. Phys. Chem.* **1996**, *100*, 16502. (b) Bytheway, I.; Wong, M. W. *Chem. Phys. Lett.* **1998**, *282*, 219.

(27) Hastie, J. W.; Hauge, R. H.; Margrave, J. L. *J. Chem. Phys.* **1969**, *51*, 2648.

Table 1. Observed and Calculated Fundamental Frequencies of $FC\div TiF_3$ ^a

approximate mode ^b	$FC\div TiF_3$		$F^{13}C\div TiF_3$
	obsd ^c	calcd (int)	calcd (int)
CTiF bend (e)		76.4 (0)	75.9 (0)
FTiF bend (e)		182.3 (4)	180.5 (2)
TiF ₃ umbrella (a ₁)		190.4 (9)	189.8 (9)
FC ₂ Ti def (e)		216.1 (21)	212.7 (22)
(FC) \div Ti stretch (a ₁)	481.7	480.3 (52)	478.0 (51)
Ti–F stretch (a ₁)	686.1	705.6 (210)	705.6 (211)
Ti–F stretch (e)	752.8	766.2 (462)	766.2 (462)
C–F stretch (a ₁)	1453.1	1470.2 (274)	1429.3 (262)

^a B3LYP//6-311+G(2d)/SDD level of theory. All frequencies are unscaled and in cm^{-1} , and computed infrared intensities are in km/mol . ^bMode symmetries for C_{3v} molecule. ^cArgon matrix.

Table 2. Observed and Calculated Fundamental Frequencies of $CiC\div TiCl_3$ ^a

approximate mode ^b	$CiC\div TiCl_3$		$Cl^{13}C\div TiCl_3$	
	obsd ^c	calcd (int)	obsd ^c	calcd (int)
CTiCl bend (e)		51.1 (0)		51.0 (0)
CiTiCl bend (e)		111.7 (0)		111.5 (0)
TiCl ₃ umbrella (a ₁)		112.6 (1)		112.4 (1)
CiC ₂ Ti def (e)		218.5 (2)		211.4 (2)
(CiC) \div Ti stretch (a ₁)		346.8 (0)		346.5 (0)
Ti–Cl stretch (a ₁)	<i>d</i>	435.8 (125)	<i>d</i>	435.8 (125)
Ti–Cl stretch (e)	487.0	481.6 (288)	487.0	481.6 (287)
C–Cl stretch (a ₁)	1151.5	1133.6 (74)	1114.1	1095.9 (69)

^a B3LYP//6-311+G(2d)/SDD level of theory. All frequencies are unscaled and in cm^{-1} , and computed infrared intensities are in km/mol . ^bMode symmetries for C_{3v} molecule. ^cArgon matrix. ^dAbsorption below our spectral limits.

this instance, carbon-13 isotopic substitution and natural abundance chlorine isotopes were employed to confirm the mode assignments as Ti–Cl and C–Cl stretching modes, respectively.¹³ Two possible products are again likely candidates. The $CCl_2=TiCl_2$ species must be considered, as analogous $CH_2=TiHCl$ and $CH_2=TiCl_2$ complexes have been formed previously.^{12,28} However, the possible singlet $CCl_2=TiCl_2$ methyldiene complex was predicted to have strong infrared absorptions at 435.4, 506.0, 739.4, and 939.3 cm^{-1} . Since the product C–Cl stretching mode is at 1151.5 cm^{-1} , the spectrum cannot be assigned to the $CCl_2=TiCl_2$ species. The predicted absorptions of the other possible triplet $CiC\div TiCl_3$ species (Table 2) are in good agreement with experiment. Hence, the observed spectrum is assigned to this electron-deficient methyldiene complex. In addition, we observe small amounts of $TiCl_4$ in our spectra at 503 cm^{-1} and $TiCl_3$ at 497 cm^{-1} , indicating that intermediates along the $Ti + CCl_4 \rightarrow TiCl_4 + C$ reaction pathway are possible complexes frozen in our inert matrix.²¹ We also observe chlorocarbon transient species such as the CCl_3 radical from laser-plume photochemistry of the precursor.^{15a,c}

Zr + CF₄. Laser-ablated zirconium atoms react with tetrafluoromethane to produce a single reaction product with infrared absorptions at 648.4, 656.8, and 1413.7 cm^{-1} . All three absorptions increased in unison on UV irradiation (Figure 2) and can be assigned to a single reaction product. The upper absorption at 1413.7 cm^{-1} is almost 40 cm^{-1} below the C–F stretching mode of the $FC\div TiF_3$ complex. The two lower absorptions are between the strong Zr–F stretching modes of ZrF_4 at 668 cm^{-1} and ZrF_2 at 633.5 cm^{-1} .^{29,30}

(28) Cho, H.-G.; Andrews, L. *Inorg. Chem.* **2005**, *44*, 979 (Ti + CH_3Cl).

(29) Büchler, A.; Berkowitz-Mattuck, J. B.; Dugre, D. H. *J. Chem. Phys.* **1961**, *34*, 2202.

(30) Hauge, R. H.; Margrave, J. L. *High Temp. Sci.* **1973**, *5*, 89.

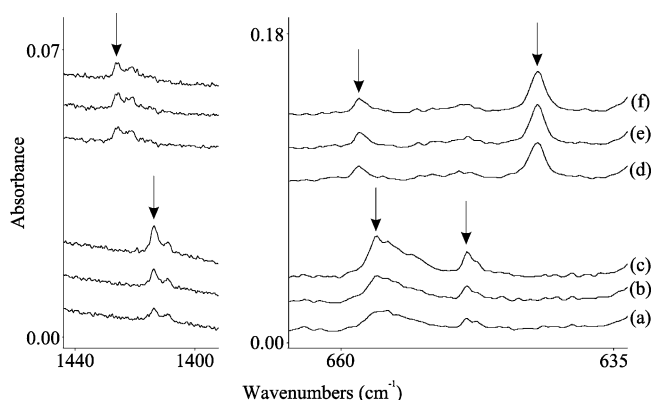


Figure 2. Infrared spectra in the 1440–1390 and 665–635 cm^{-1} regions taken after (a) laser-ablated zirconium atoms were reacted with 0.5% CF_4/Ar during condensation at 8 K for 1 h, and the resulting matrix was subjected to (b) irradiation with light $\lambda > 290$ nm and (c) irradiation with $\lambda > 220$ nm, and when (d) laser-ablated hafnium atoms were reacted with 0.5% CF_4/Ar during condensation at 8 K for 1 h, and the resulting matrix was subjected (e) irradiation with light $\lambda > 290$ nm and (f) irradiation with $\lambda > 220$ nm. Arrows indicate product absorptions.

Table 3. Observed and Calculated Fundamental Frequencies of $FC\div ZrF_3$ and $FC\div HfF_3$ ^a

approximate mode ^b	$FC\div ZrF_3$		$FC\div HfF_3$	
	obsd ^c	calcd (int)	obsd ^c	calcd (int)
CMF bend (e)		91.9 (2)		92.1 (4)
FMF bend (e)		161.4 (20)		163.5 (14)
MF ₃ umbrella (a ₁)		163.0 (14)		156.7 (20)
FCM def (e)		204.3 (23)		191.8 (24)
(FC) \div M stretch (a ₁)		420.8 (81)		397.0 (72)
M–F stretch (a ₁)	648.4	637.0 (120)	641.9	628.9 (282)
M–F stretch (e)	656.8	655.5 (374)	658.2	635.4 (80)
C–F stretch (a ₁)	1413.7	1433.9 (192)	1426.5	1438.1 (162)

^a B3LYP//6-311+G(2d)/SDD level of theory. All frequencies are in cm^{-1} , and computed infrared intensities are in km/mol . ^bMode symmetries for C_{3v} molecule. ^cArgon matrix. ^dAbsorption below our spectral limits.

The possible singlet $CF_2=ZrF_2$ complex is predicted to be 150 $kcal/mol$ more stable than the sum of the individual zirconium and CF_4 precursors. However, this complex is computed to have two strong C–F stretching modes at 1041.2 and 1207.7 cm^{-1} , and no appropriate absorptions were observed. Conserving the singlet multiplicity, a third fluorine atom can transfer to the zirconium center, forming a bent $FC-ZrF_3$ complex, which is 13 $kcal/mol$ lower in energy than the methyldiene. This species is predicted to have strong infrared absorptions at 642.2, 648.8, and 1388.6 cm^{-1} . However, the triplet $FC\div ZrF_3$ analogue is an additional 24 $kcal/mol$ lower in energy, and the predicted spectrum (637.0, 656.8, and 1433.9 cm^{-1}) matches the observed absorptions even better (Table 3) particularly since the calculated C–F mode is expected to fall above the observed value.^{13,26} Hence the observed spectrum is assigned to the $FC\div ZrF_3$ complex.

Hf + CF₄. Carbon tetrafluoride reacts with hafnium atoms to produce a single reaction product with infrared absorptions at 641.9, 658.2, and 1426.5 cm^{-1} (Figure 2). The upper absorption falls between the C–F stretching modes of the $FC\div TiF_3$ and $FC\div ZrF_3$ complexes, and the two lower absorptions are appropriate for Hf–F stretching modes, as HfF_4 has been observed at 645 cm^{-1} .²⁹

The singlet $CF_2=HfF_2$ species is calculated to be 144 $kcal/mol$ lower in energy than the sum of the precursors. However,

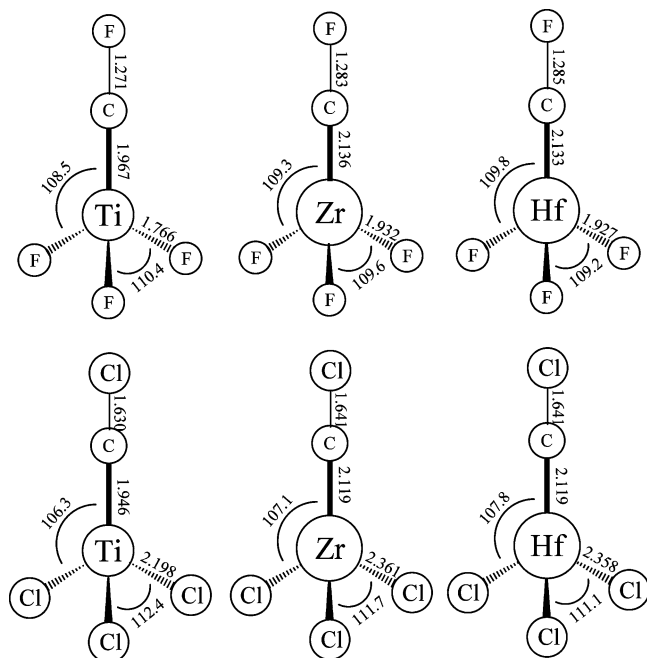


Figure 3. Optimized geometries of the $FC\div MF_3$ and $ClC\div MCl_3$ complexes computed with C_{3v} symmetry at the B3LYP//6-311+G-(2d)/SDD level of theory. Bond lengths are in angstroms and angles are in degrees.

the infrared spectrum is predicted to have two C–F stretching absorptions at 1041.4 and 1200.8 cm^{-1} , and these absorptions are not observed. The next intermediate is the singlet $FC-HfF_3$ species, which is 24 kcal/mol lower in energy. This complex is expected to relax to triplet $FC\div HfF_3$, which has C_{3v} symmetry and is 23 kcal/mol lower in energy than the singlet analogue. The predicted infrared absorptions for this species (strong infrared absorptions at 628.9, 635.4, and 1428.1 cm^{-1}) match those observed within the limits expected for DFT (Table 3). Hence, the observed spectrum is assigned to the triplet $FC\div HfF_3$ complex.

The structures calculated for the $FC\div MF_3$ product species are illustrated in Figure 3, where bonding trends, particularly the common C–F bond length, can be compared.

Zr and Hf + CCl_4 . Zirconium reacted with carbon tetrachloride to produce a product with a weak band at 1131.8 cm^{-1} and a strong infrared absorption at 419.2 cm^{-1} , which increased together on UV irradiation, as shown in Figure 4. The weak band shifted to 1195.0 cm^{-1} with carbon-13, but the strong absorption showed no isotopic shift, which identifies C–Cl and Zr–Cl stretching modes, respectively. Hafnium is more difficult to evaporate, and no product absorptions were observed with hafnium. We will discuss possible product species and base our assignment in part on relative calculated product energies.

The $CCl_2=ZrCl_2$ complex lies 180 kcal/mol lower in energy than the sum of the reactant energies. Our theoretical computations on this species find only one Zr–Cl stretching mode to be within our spectral range at 418.7 cm^{-1} , which agrees fairly well with the observed absorption at 419.2 cm^{-1} . However, this species is also predicted to have two C–Cl stretching modes, with the strongest (139 km/mol) at 707.0 cm^{-1} . This is a clean region in the infrared spectrum where no product absorption was observed. The bent singlet $ClC-ZrCl_3$ complex is 14 kcal/mol lower in energy than the methyldene complex, and the symmetrical triplet $ClC\div ZrCl_3$ complex is an additional 21 kcal/mol lower in energy. For the singlet complex, all vibrational modes are predicted to fall below our spectral limits with the

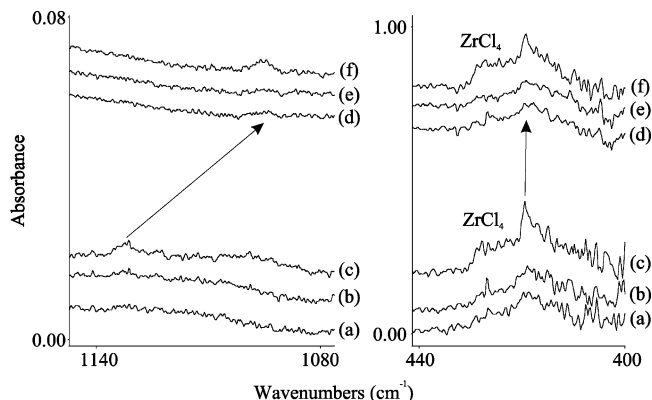


Figure 4. IR spectra in the 1140–1080 and 440–400 cm^{-1} regions of the spectra taken after (a) laser-ablated zirconium atoms were reacted with 0.5% CCl_4/Ar , (b) the matrix sample was irradiated at $\lambda > 290$ nm and (c) at $\lambda > 220$ nm, and after (d) zirconium atoms were reacted with 0.5% $^{13}CCl_4/Ar$ (90% ^{13}C enriched), (e) the matrix sample was irradiated at $\lambda > 290$ nm and (f) at $\lambda > 220$ nm. The product absorptions are marked with arrows.

exception of the one C–Cl stretching peak at 1119.2 cm^{-1} (with IR intensity 59 km/mol). For the triplet complex, a Zr–Cl stretching mode calculated at 408.7 cm^{-1} is in reasonable agreement with experiment (Table 4) and the C–Cl stretching mode is computed at 1100.9 cm^{-1} (28 km/mol). Hence it is most likely that the reaction product observed at 1131.8 and 419.2 cm^{-1} is the lower energy triplet $ClC\div ZrCl_3$ complex. Our calculation overestimates the C–F stretching mode and underestimates the C–Cl stretching mode for the titanium product species.¹³ We note that the $ZrCl_4$ antisymmetric stretching fundamental has been observed in the 250 °C gas-phase IR spectrum at 423 cm^{-1} .²⁹ Our weak 427 cm^{-1} argon matrix band is probably due to $ZrCl_4$.

$CCl_2=HfCl_2$ is predicted by our theoretical computations to be 174 kcal/mol more stable than the CCl_4 and Hf atom reactants. For this complex, the strongest infrared active mode (C–Cl stretching; 129 km/mol) is predicted at 705.4 cm^{-1} . Again this is a clean region of the spectrum, and no band was observed. The singlet $ClC-HfCl_3$ species is 22 kcal/mol lower in energy than the double-bonded $CCl_2=HfCl_2$ complex. For this species, the only absorption that is within our spectral range is the C–Cl stretching mode, which is predicted at 1120.3 cm^{-1} (46 km/mol). The last complex that needs to be considered is the triplet $ClC\div HfCl_3$, which is an additional 22 kcal/mol lower in energy. For this species, the C–Cl stretching mode is predicted (Table 4) at 1107.5 cm^{-1} with lower intensity (19 km/mol). Although no absorptions were detected, it is most likely that the lowest energy triplet complex is formed in low yield but not observed here. Our prediction for the strongest mode of $ClC\div HfCl_3$ (375 cm^{-1}) is below the 393 cm^{-1} absorption²⁹ reported for $HfCl_4$, and we cannot observe these low-frequency absorptions. For comparison, we display the structures of the lowest energy triplet complexes in Figure 3.

Ti + CF_2Cl_2 . Titanium atoms react with CF_2Cl_2 to produce four sets of new absorptions. Product peaks at 486.9, 730.7, and 1453.1 cm^{-1} decreased dramatically after radiation with $\lambda > 290$ nm and are labeled A in Figure 5. Absorptions at 466.9, 705.9, and 755.2 cm^{-1} decreased slightly on exposure to light with $\lambda > 290$ nm, but increased on full-arc photolysis ($\lambda > 220$ nm), and are denoted B in Figure 5. Two absorptions at 646.9 and 743.6 cm^{-1} increased markedly on photolysis with a Pyrex filter ($\lambda > 290$ nm), decreased slightly on full-arc irradiation, and are labeled C. Finally, stable absorptions at 508.9

Table 4. Observed and Calculated Fundamental Frequencies of $CIC\div ZrCl_3$ and $CIC\div HfCl_3$ ^a

approximate mode ^b	$CIC\div ZrCl_3$		$C^{13}C\div ZrCl_3$		$CIC\div HfCl_3$	
	obsd ^c	calcd (int)	obsd ^c	calcd (int)	obsd ^c	calcd (int)
CMCl bend (e)		53.2 (0)		53.2 (0)		52.4 (0)
MCl ₃ umbrella (a ₁)		94.2 (3)		94.1 (3)		90.9 (4)
CIMCl bend (e)		94.9 (2)		94.9 (2)		94.1 (2)
CICM def (e)		199.6 (6)		192.7 (6)		193.4 (8)
(CIC) \div M stretch (a ₁)		321.7 (22)		321.1 (22)		302.8 (41)
M–Cl stretch (a ₁)	<i>d</i>	374.0 (87)	<i>d</i>	373.9 (87)	<i>d</i>	363.3 (40)
M–Cl stretch (e)	419.2	408.7 (238)	419.2	408.7 (238)	<i>d</i>	375.0 (176)
C–Cl stretch (a ₁)	1131.8	1100.9 (28)	1095.0	1063.9 (27)		1107.5 (19)

^a B3LYP//6-311+G(2d)/SDD level of theory. All frequencies are unscaled and in cm^{-1} , and computed infrared intensities are in km/mol . ^b Mode symmetries for C_{3v} molecule. ^c Argon matrix. ^d Absorption below our spectral limit.

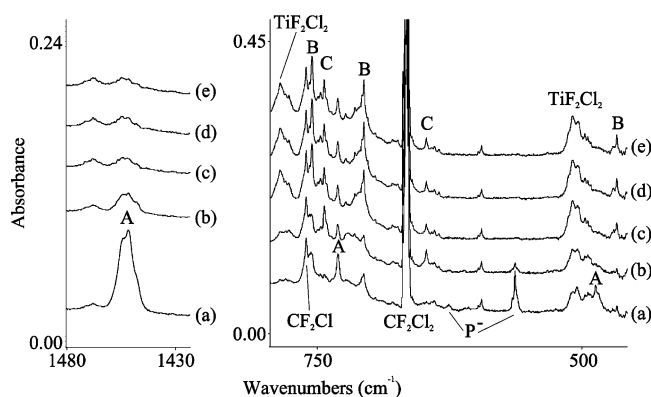


Figure 5. Infrared spectra in the 1480–1425 and 800–450 cm^{-1} regions taken after (a) laser-ablated titanium atoms were reacted with 1.0% CF_2Cl_2/Ar during condensation at 8 K for 1 h, and the resulting matrix was subjected to (b) irradiation with light $\lambda > 290$ nm, (c) irradiation with $\lambda > 220$ nm, (d) annealing to 30 K, and (e) irradiation with $\lambda > 470$ nm. Product absorptions labeled A belong to the $FC\div TiFCl_2$ complex, B peaks are assigned to the $CIC\div TiF_2Cl$ species, and the identity of C peaks is not resolved. Common precursor products CF_2Cl radical and parent anion (P^-) are labeled in the figure; see ref 15.

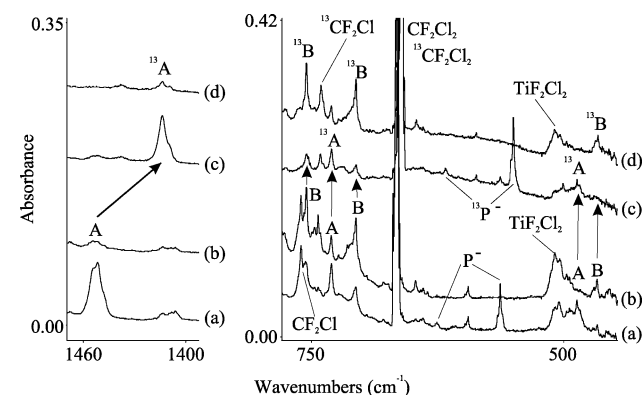


Figure 6. IR spectra in the 1470–1390 and 780–450 cm^{-1} regions of the spectra taken after (a) laser-ablated titanium atoms were reacted with 1.0% CF_2Cl_2/Ar , and (b) the matrix sample was photolyzed with $\lambda > 220$ nm, and after (c) titanium atoms were reacted with 1.0% $^{13}CF_2Cl_2/Ar$ (90% ^{13}C enriched), and (d) the matrix sample was photolyzed with $\lambda > 220$ nm. Common precursor products CF_2Cl radical and parent anion (P^-) are labeled in the figure; see ref 15.

and 785.4 cm^{-1} increased on full-arc irradiation and are labeled TiF_2Cl_2 in Figure 3.

The upper A absorption at 1453.1 cm^{-1} shifts to 1413.8 cm^{-1} on ^{13}C isotopic substitution, indicative of a C–F stretching mode (Figure 6). The next absorption at 730.7 cm^{-1} does not shift on carbon-13 substitution, and the last A peak at 486.9 cm^{-1} shows

Table 5. Observed and Calculated Fundamental Frequencies of $FC\div TiFCl_2$ ^a

approximate mode	$FC\div TiFCl_2$		$F^{13}C\div TiFCl_2$	
	obsd ^b	calcd (int)	obsd ^b	calcd (int)
CTiCl bend		62.9 (0)		62.9 (0)
CTiF bend		68.0 (0)		67.8 (0)
CTiCl bend		113.3 (1)		113.1 (1)
FTiCl bend		146.2 (2)		146.0 (2)
TiFCl ₂ umbrella		151.3 (3)		150.7 (3)
FCTi def		212.2 (2)		206.5 (2)
FCTi def		235.4 (0)		228.0 (1)
Ti–Cl stretch	<i>c</i>	399.3 (19)	<i>c</i>	398.3 (18)
Ti–Cl stretch	486.9	482.2 (165)	486.6	482.1 (165)
(FC) \div Ti stretch	(495)	503.0 (102)	<i>d</i>	501.5 (102)
Ti–F stretch	730.7	744.5 (190)	730.7	744.5 (190)
C–F stretch	1453.1	1472.4 (439)	1413.8	1431.5 (420)

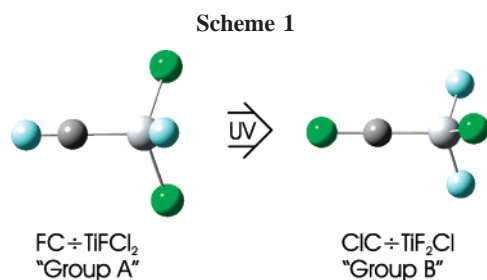
^a B3LYP//6-311+G(2d)/SDD level of theory. All frequencies are unscaled and in cm^{-1} , and computed infrared intensities are in km/mol . ^b Argon matrix. ^c Absorption below our spectral limit. ^d Absorption in the 490–495 cm^{-1} region shows the photochemical behavior of this species.

only a 0.3 cm^{-1} ^{13}C red shift. These two product absorptions are in the regions of Ti–F and Ti–Cl stretching modes, respectively. (The observed Ti–F stretching mode is halfway between the two Ti–F stretching modes of the $FC\div TiF_3$ species, and the Ti–Cl mode is almost identical to the antisymmetric Ti–Cl stretching mode of the $CIC\div TiCl_3$ complex.) These three product peaks identify the reaction product as either $CFCl=TiFCl$ or $FC\div TiFCl_2$. The singlet $CFCl=TiFCl$ methyldene is 136 kcal/mol lower in energy than the sum of the CF_2Cl_2 and titanium atom reactants, and the triplet analogue has the same energy. However, for the singlet complex the C–F stretching mode is predicted to be at 1168.9 cm^{-1} , nearly 285 cm^{-1} lower than the observed peak. The triplet $CFCl=TiFCl$ complex has the C–F stretching mode at 1200.3 cm^{-1} , which is still too far below the observed peak to warrant assigning the A absorptions to either of these complexes. The bent singlet $FC=TiFCl_2$ complex is predicted to be only 1 kcal/mol higher in energy than the methyldene complex. Here the C–F stretching mode is predicted higher at 1306.4 cm^{-1} . Once the third halogen transfers to the titanium center, spin relaxation to the lower energy triplet $FC\div TiFCl_2$ complex occurs. The triplet complex is 17 kcal/mol lower in energy than the singlet analogue (152 kcal/mol below $Ti + CF_2Cl_2$). Here the C–F stretching mode is predicted at 1472.4 cm^{-1} with a 40.9 cm^{-1} ^{13}C isotopic shift, in excellent agreement with the 1453.1 cm^{-1} observed band and 39.3 cm^{-1} shift. The Ti–F and Ti–Cl stretches are predicted at 744.5 and 482.2 cm^{-1} , respectively, also in good agreement with the observed peaks (Table 5). The broad 495 cm^{-1} absorption is probably due to the symmetric (FC) \div Ti stretch calculated at 503.0 cm^{-1} . The second Ti–Cl stretching mode is predicted at 399.3 cm^{-1} , which is too low for us to observe here. Hence the observed A absorptions are assigned to the

Table 6. Observed and Calculated Fundamental Frequencies of $\text{CIC}\div\text{TiF}_2\text{Cl}$ ^a

approximate mode	$\text{CIC}\div\text{TiF}_2\text{Cl}$		$\text{Cl}^{13}\text{C}\div\text{TiF}_2\text{Cl}$	
	obsd ^b	calcd (int)	obsd ^b	calcd (int)
CTiCl bend		56.5 (0)		56.3 (0)
CTiF bend		61.8 (0)		61.3 (0)
FTiCl bend		149.4 (2)		149.4 (2)
TiF ₂ Cl umbrella		155.7 (2)		154.7 (2)
FTiF bend		179.8 (4)		179.4 (4)
CiCTi bend		217.5 (5)		212.0 (5)
CiCTi def		223.1 (4)		217.3 (4)
(CIC) \div Ti stretch	<i>c</i>	383.9 (29)	<i>c</i>	383.6 (29)
Ti–Cl stretch	466.9	467.0 (178)	466.0	466.9 (178)
Ti–F stretch	705.9	724.7 (231)	705.9	724.6 (231)
Ti–F stretch	755.2	768.3 (203)	755.2	768.3 (202)
C–Cl stretch	<i>d</i>	1133.9 (29)	<i>d</i>	1096.3 (26)

^a B3LYP//6-311+G(2d)/SDD level of theory. All frequencies are unscaled and in cm^{-1} , and computed infrared intensities are in km/mol . ^b Argon matrix. ^c Absorption below our spectral limit. ^d Peak is hidden behind precursor absorption.



triplet $\text{FC}\div\text{TiFCl}_2$ complex, which is the only complex we found with such a high frequency and very intense C–F stretching mode.

The three B absorptions all show practically no carbon-13 isotopic shift (Figure 6), and hence these vibrational modes have no carbon character. The two upper absorptions at 755.2 and 705.9 cm^{-1} are slightly above the Ti–F stretching modes of the $\text{FC}\div\text{TiF}_3$ complex. Hence they are assigned to Ti–F stretching modes. The lower absorption at 466.9 cm^{-1} is near the observed Ti–Cl stretching mode of the $\text{CIC}\div\text{TiCl}_3$ complex, and hence it is assigned to a Ti–Cl mode. The observation of these three vibrational modes (two Ti–F and one Ti–Cl stretching) leads to the assignment of the triplet $\text{CIC}\div\text{TiF}_2\text{Cl}$ complex with confidence. Computations led to a stable triplet complex 163 kcal/mol lower in energy than the sum of the titanium atom and CF_2Cl_2 reactants. The three observed peaks agree well with the predicted infrared spectrum (Table 6). Note that the only other absorption calculated to be above the lower limit of our spectrometer is the C–Cl stretching mode, which is predicted to fall behind a CF_2Cl_2 precursor absorption. It is of interest to note here that the $\text{FC}\div\text{TiFCl}_2$ complex formed on deposition is converted into the $\text{CIC}\div\text{TiF}_2\text{Cl}$ species on UV irradiation, as summarized in Scheme 1. Surely this transformation must occur through a bridge-bonded transition state. The scheme also serves to illustrate the triplet state product structures.

Two other absorptions at 508.9 and 785.4 cm^{-1} increased on irradiation like TiF_4 and TiCl_4 in our experiments with CF_4 and CCl_4 . The above bands correlate with the calculated spectra³¹ for TiF_2Cl_2 and are assigned accordingly.

The two weaker C absorptions at 646.9 and 743.6 cm^{-1} show 0.7 and 3.0 cm^{-1} ¹³C isotopic shifts, respectively, which can

be assigned to mostly Ti–F stretching modes. Hence they could arise from either triplet $\text{CCl}_2\text{--TiF}_2$, singlet $\text{CCl}_2\text{=TiF}_2$, or singlet $\text{CIC--TiF}_2\text{Cl}$ intermediate species. Our calculations find these complexes 143, 144, and 145 kcal/mol lower in energy than the reactants, respectively. The two Ti–F stretching modes of the triplet $\text{CCl}_2\text{--TiF}_2$ complex are predicted to be strong infrared absorbers at 675.2 and 760.6 cm^{-1} and to show 0.9 and 0.0 cm^{-1} ¹³C isotopic shifts, respectively. However, this complex also has a strong antisymmetric C–Cl stretching mode calculated at 771.6 cm^{-1} , which is not observed. Next, the singlet $\text{CCl}_2\text{=TiF}_2$ methyldene complex is predicted to have two strong Ti–F stretching modes at 668.5 and 776.9 cm^{-1} (1.2 and 1.0 cm^{-1} ¹³C shift, respectively), which are again in good agreement with the two observed peaks. Again a stronger antisymmetric C–Cl stretching mode is predicted lower at 737.2 cm^{-1} . This peak again is not observed, but it could be hidden behind the CF_2Cl_2 precursor absorption at 660–670 cm^{-1} . As all other absorptions for this species are predicted to be below our spectral limits or too weak to be observed, it is possible that the group C absorptions correspond to the singlet $\text{CCl}_2\text{=TiF}_2$ complex. The third possible product is the bent singlet $\text{CIC--TiF}_2\text{Cl}$ complex. Here the two Ti–F stretching modes are predicted at 721.7 and 768.6 cm^{-1} (0.1 and 0.0 cm^{-1} ¹³C isotopic shifts, respectively), which again are in fairly good agreement with experiment. The next two strongest bands are calculated at 452.8 (Ti–Cl stretch) and 987.7 cm^{-1} (C–Cl stretch). Although the Ti–Cl stretching mode could fall below our spectral limits, the C–Cl stretching mode predicted at 987.7 cm^{-1} should appear in a clean region of the spectrum. Hence, the C absorptions cannot belong to the singlet $\text{CIC--TiF}_2\text{Cl}$ complex. In addition, we believe it is more likely that the rigid argon matrix would prevent α -Cl transfer rather than singlet to triplet spin relaxation in the formation of triplet $\text{CIC}\div\text{TiF}_2\text{Cl}$. It is also quite likely that the group C absorptions correspond to an intermediate species between the conversion of the triplet $\text{FC}\div\text{TiFCl}_2$ and $\text{CIC}\div\text{TiF}_2\text{Cl}$ complexes, which we did not locate theoretically. Hence, the weak group C absorptions remain unidentified.

Zr + CF_2Cl_2 . Zirconium atoms reacted with CF_2Cl_2 to produce product absorptions that can be separated into three groups based on product behavior. Two group A absorptions at 656.8 and 1428.4 cm^{-1} increased in intensity on photolysis with $\lambda > 470$ nm and with $\lambda > 290$ nm, decreased in intensity after exposure to radiation of $\lambda > 220$ nm, and remained unchanged after annealing to 30 K (Figure S1 in Supporting Information). This absorption red shifts 39.2 cm^{-1} upon carbon-13 isotopic substitution, and it can be assigned to a C–F stretching mode (Figure 7). Notice that this mode is 14.7 cm^{-1} higher than the analogous mode of the triplet $\text{FC}\div\text{ZrF}_3$ complex. This high C–F stretching mode was diagnostic for the formation of triplet $\text{FC}\div\text{TiF}_3$, as no other molecule was found to have such a high C–F vibrational frequency.¹³ Hence, it is probable that this group A absorption belongs to triplet $\text{FC}\div\text{ZrFCl}_2$. Computations on this complex led to a structure 198 kcal/mol lower in energy than the sum of zirconium atom and CF_2Cl_2 precursors, which is the lowest energy structure we could find with a C–F bond. The C–F stretching mode for this $\text{FC}\div\text{ZrFCl}_2$ complex is predicted at 1439.3 cm^{-1} (40.1 cm^{-1} ¹³C shift), which accurately reproduces the 1428.4 cm^{-1} (39.2 cm^{-1} carbon-13 shift) value observed (Table 7). The next strongest predicted mode for this complex (Zr–F stretching, 650.2 cm^{-1}) is near the 656.8 cm^{-1} band. All other modes computed for the $\text{FC}\div\text{ZrFCl}_2$ complex are calculated at or below our spectral

(31) Bauschlicher Jr., C. W.; Taylor, P. R.; Komornicki, A. J. *Chem. Phys.* **1990**, *92*, 3982.

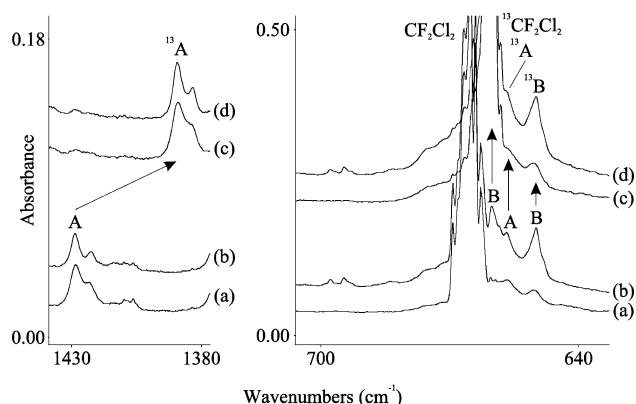


Figure 7. IR spectra in the 1440–1380 and 700–630 cm^{-1} regions of the spectra taken after (a) laser-ablated zirconium atoms were reacted with 1.0% $\text{CF}_2\text{Cl}_2/\text{Ar}$, and (b) the matrix sample was photolyzed with $\lambda > 220$ nm, and after (c) zirconium atoms were reacted with 1.0% $^{13}\text{CF}_2\text{Cl}_2/\text{Ar}$ (90% ^{13}C enriched), and (d) the matrix sample was photolyzed with $\lambda > 220$ nm.

Table 7. Observed and Calculated Fundamental Frequencies of $\text{FC}\div\text{ZrFCl}_2$ ^a

approximate mode	$\text{FC}\div\text{ZrFCl}_2$		$\text{F}^{13}\text{C}\div\text{ZrFCl}_2$	
	obsd ^b	calcd (int)	obsd ^b	calcd (int)
CZrCl bend		68.8 (0)		68.7 (0)
CZrF bend		79.7 (1)		79.7 (1)
ClZrCl bend		96.8 (2)		96.7 (2)
FZrCl bend		122.8 (4)		122.8 (4)
ZrFCl ₂ umbrella		137.3 (6)		137.0 (6)
FCZr def		211.2 (4)		204.5 (4)
FCZr def		224.4 (2)		217.0 (2)
Zr–Cl stretch		374.8 (22)		374.0 (20)
Zr–Cl stretch		409.8 (131)		409.7 (130)
(FC) \div Zr stretch	c	426.9 (101)	c	424.5 (101)
Zr–F stretch	656.8	650.2 (151)	656.8	650.2 (151)
C–F stretch	1428.4	1439.3 (294)	1389.2	1399.2 (284)

^a B3LYP//6-311+G(2d)/SDD level of theory. All frequencies are unscaled and in cm^{-1} , and computed infrared intensities are in km/mol . ^b Argon matrix. ^c Absorption below our spectral limit.

lower limit. Hence, the group A absorptions are assigned to the triplet $\text{FC}\div\text{ZrFCl}_2$ complex.

Two group B absorptions were observed at 649.7 and 660.1 cm^{-1} . These absorptions increased slightly on photolysis with $\lambda > 290$ nm, increased by more than a factor of 4 when exposed to light with $\lambda > 220$ nm, and remained unchanged in intensity after annealing to 30 K. The lower absorption showed no carbon-13 isotopic shift, the upper B peak probably shows no isotopic shift (the carbon-13 counterpart is hidden behind the $^{13}\text{CF}_2\text{Cl}_2$ precursor peak), and both absorptions can be assigned to Zr–F stretching modes. The presence of two Zr–F stretching modes and the intensity of the absorptions indicate that the reaction product is either the singlet $\text{CCl}_2=\text{ZrF}_2$ methyldene complex or the triplet $\text{ClC}\div\text{ZrF}_2\text{Cl}$ complex. These two molecules are predicted to be 172 and 207 kcal/mol lower in energy than the sum of the individual reactants, respectively. The singlet $\text{CCl}_2=\text{ZrF}_2$ has two Zr–F stretching modes at 613.2 and 650.8 cm^{-1} , which are below the observed bands. In addition, two C–Cl stretching modes are predicted at 704.9 and 932.1 cm^{-1} . The lower C–Cl stretching mode should be quite intense, but it was not observed in our experiment. The triplet $\text{ClC}\div\text{ZrF}_2\text{Cl}$ complex is predicted to have two Zr–F stretching modes at 642.1 and 657.3 cm^{-1} (Table 8), accurately reproducing the observed bands. The only other absorption above our spectral limit (C–Cl stretching) is predicted to be weak (5% of

Table 8. Observed and Calculated Fundamental Frequencies of $\text{ClC}\div\text{ZrF}_2\text{Cl}$ ^a

approximate mode	$\text{ClC}\div\text{ZrF}_2\text{Cl}$		$\text{Cl}^{13}\text{C}\div\text{ZrF}_2\text{Cl}$	
	obsd ^b	calcd (int)	obsd ^b	calcd (int)
CZrCl bend		58.1 (0)		58.0 (0)
CZrF bend		64.1 (0)		63.8 (0)
FZrCl bend		124.8 (4)		124.8 (4)
ZrF ₂ Cl umbrella		134.2 (7)		133.7 (7)
FZrF bend		152.7 (8)		152.6 (8)
ClCZr def		193.9 (9)		188.1 (9)
ClCZr def		197.1 (8)		191.0 (8)
(ClC) \div Zr stretch		331.0 (58)		330.3 (58)
Zr–Cl stretch	c	398.7 (122)	c	398.6 (122)
Zr–F stretch	649.7	642.1 (161)	649.7	642.1 (162)
Zr–F stretch	660.1	657.3 (170)	d	657.3 (170)
C–Cl stretch		1099.1 (9)		1062.2 (9)

^a B3LYP//6-311+G(2d)/SDD level of theory. All frequencies are unscaled and in cm^{-1} , and computed infrared intensities are in km/mol . ^b Argon matrix. ^c Absorption below our spectral limit. ^d Absorption hidden by strong CF_2Cl_2 precursor.

the Zr–F stretching modes), and it was not observed. Hence, we assign the group B absorptions to the triplet $\text{ClC}\div\text{ZrF}_2\text{Cl}$ complex.

The two group C absorptions at 694.6 and 697.7 cm^{-1} increased slightly with $\lambda > 290$ nm and more upon full-arc photolysis ($\lambda > 220$ nm) (Figure 5). They show 0.0 and 0.1 cm^{-1} ^{13}C isotopic shifts, respectively, and can be assigned to Zr–F stretching modes. Hence three higher energy species are possible. The triplet $\text{CCl}_2=\text{ZrF}_2$, singlet $\text{CCl}_2=\text{ZrF}_2$, and singlet $\text{ClC}\div\text{ZrF}_2\text{Cl}$ complexes lie 166, 172, and 186 kcal/mol lower in energy than the sum of the zirconium atom and CF_2Cl_2 precursors, respectively. The triplet $\text{CCl}_2=\text{ZrF}_2$ complex is computed to have Zr–F stretching modes at 623.9 and 656.4 cm^{-1} , which are significantly lower than the observed peaks. In addition, two C–Cl stretching modes are predicted at 758.0 and 887.1 cm^{-1} . The lower C–Cl mode is quite intense (164 km/mol), but was not observed in experiment.

The possible singlet $\text{CCl}_2=\text{ZrF}_2$ species is predicted to have Zr–F stretching modes at 613.2 and 650.8 cm^{-1} , which again are considerably lower than the observed peaks. Also, a strong C–Cl stretching mode is predicted at 704.9 cm^{-1} , which is not observed. The last possible high-energy complex we considered was the singlet $\text{ClC}\div\text{ZrF}_2\text{Cl}$ complex. Here the two Zr–F stretching modes are predicted at 635.1 and 647.6 cm^{-1} , which are still lower than the observed peaks. However, no other absorptions are predicted to be strong infrared absorbers and to fall within our spectral limits. Hence, we are unable to assign the weak group C absorptions.

Hf + CF_2Cl_2 . Laser-ablated hafnium atoms react with CF_2Cl_2 to produce product absorptions, which can be separated into three categories. Two group A absorptions at 650.6 and 1439.2 cm^{-1} increased in intensity after photolysis with $\lambda > 290$ nm and $\lambda > 220$ nm, remained nearly unchanged after annealing to 30 K, and decreased on a final full-arc photolysis with $\lambda > 220$ nm (Figure S2 in Supporting Information). The upper absorption shifts to 1399.4 cm^{-1} upon carbon-13 isotopic substitution (Figure 8) and can be assigned to the C–F stretching mode. Notice that this absorption is 12.7 cm^{-1} higher than the C–F stretching mode of the triplet $\text{FC}\div\text{HfF}_3$ complex. Computations on the possible $\text{FC}\div\text{HfFCl}_2$ complex led to a structure 201 kcal/mol lower in energy than the sum of Hf atom and CF_2Cl_2 precursors (the lowest energy structure we found with a C–F bond). This complex was predicted to have one C–F stretching mode at 1442.5 cm^{-1} (40.5 cm^{-1} ^{13}C isotopic shift), in excellent agreement with the observed

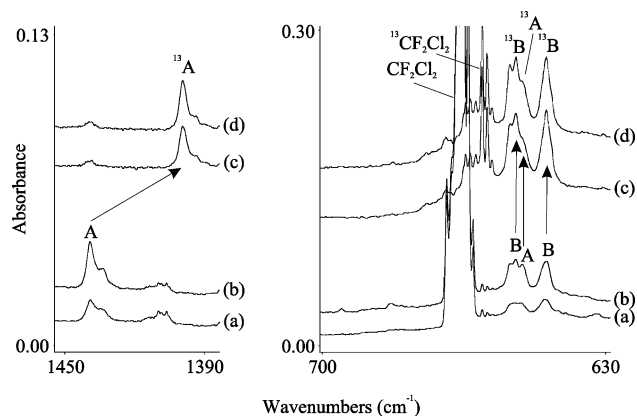


Figure 8. IR spectra in the 1450–1390 and 700–630 cm^{-1} regions of the spectra taken after (a) laser-ablated hafnium atoms were reacted with 1.0% $\text{CF}_2\text{Cl}_2/\text{Ar}$, and (b) the matrix sample was photolyzed with $\lambda > 220$ nm, and after (c) hafnium atoms were reacted with 0.25% $^{13}\text{CF}_2\text{Cl}_2/\text{Ar}$ (90% ^{13}C enriched), and (d) the matrix sample was photolyzed with $\lambda > 220$ nm.

absorption (Table S1 in Supporting Information). The only other absorption calculated to be in our experimental range (Hf–F stretching mode at 632.5 cm^{-1}) is observed at 650.6 cm^{-1} on the side of the stronger group B absorptions (Figure 8b). Hence, the group A absorptions are assigned to the triplet $\text{FC}\div\text{HfFCl}_2$ complex.

Group B absorptions at 644.6 and 652.2 cm^{-1} increased slightly in intensity after photolysis with a Pyrex filter ($\lambda > 290$ nm), doubled in intensity after exposure to radiation with $\lambda > 220$ nm, remained nearly unchanged on annealing to 30 K, and increased further after an additional photolysis with $\lambda > 220$ nm. Both absorptions show nearly no carbon-13 isotopic shift (Figure 8) and can be assigned to two Hf–F stretching modes. Hence, the group B absorptions probably correspond to either the singlet $\text{CCl}_2=\text{HfF}_2$ or the triplet $\text{ClC}\div\text{HfF}_2\text{Cl}$, which are predicted to be 166 and 212 kcal/mol lower in energy than the sum of the hafnium atom and CF_2Cl_2 precursors, respectively. The singlet $\text{CCl}_2=\text{HfF}_2$ complex is predicted to have two Hf–F stretching modes at 620.0 and 622.4 cm^{-1} . However, both C–Cl modes of this complex are computed to be quite intense at 709.6 and 916.9 cm^{-1} . The upper absorption would be covered by the CF_2Cl_2 precursor, but the lower C–Cl stretching mode should be observed. As it was not seen in experiment, group B absorptions probably do not correspond to this complex. The triplet $\text{ClC}\div\text{HfF}_2\text{Cl}$ complex is computed to have two Hf–F stretching modes at 629.7 and 632.1 cm^{-1} , closer to the observed bands than those predicted for the methyldene complex. The only other absorption that is calculated to fall within our spectral limits (C–Cl stretching) is predicted to be too weak to observe (Table S2 in Supporting Information). Hence, the two group B absorptions are assigned to the triplet $\text{ClC}\div\text{HfF}_2\text{Cl}$ complex.

One group C absorption observed at 683.0 cm^{-1} (0.4 cm^{-1} ^{13}C isotopic shift) increased in intensity on exposure to UV radiation. Hence, we are in search of a third reaction product with a Hf–F stretching mode. The singlet $\text{CClF}=\text{HfClF}$ and triplet $\text{CClF}-\text{HfClF}$ complexes were computed to be 159 and 161 kcal/mol lower in energy than the reactants and to have strong C–F and C–Cl stretching modes, neither of which were observed. The possible singlet $\text{CCl}_2=\text{HfF}_2$ and triplet $\text{CCl}_2-\text{HfF}_2$ complexes lie 166 and 168 kcal/mol lower in energy than the sum of the reactants. However, here both Hf–F stretching and at least one of the C–Cl stretching modes were predicted

with considerable infrared intensity. Again, however, only one absorption was observed. The singlet $\text{ClC}-\text{HfF}_2\text{Cl}$ complex (189 kcal/mol lower in energy than the reactants) is predicted to have two observable Hf–F stretching modes, and the singlet $\text{FC}-\text{HfFCl}_2$ complex (177 kcal/mol lower in energy) has only one Hf–F stretching mode, but also possesses a strong C–Cl stretching mode, which is not observed. Hence, we are unable to assign this group C absorption.

Group Trends and Bonding Considerations. The geometries of the $\text{FC}\div\text{MF}_3$ and $\text{ClC}\div\text{MCl}_3$ complexes are shown in Figure 3, and the calculated parameters are listed in Table S3 (Supporting Information). A few interesting observations merit comment. First, notice the elongation of the terminal C–X bonds as the metal atom becomes heavier, which suggests decreasing halogen conjugation with the $\text{C}\div\text{M}$ π -bonding system. The $\text{C}\div\text{M}$ bond length is shorter in the chlorine complexes than in the fluorine analogues. Also note that the Mulliken charges on the carbon-bonded halogen atoms switch between the fluorine and chlorine complexes, as Cl conjugates more effectively with carbon and the $\text{C}\div\text{M}$ π system than F. Hence, it appears that decreasing the electronegativity of the halogen atom increases the $\text{C}\div\text{M}$ bond strength. This probably arises from contraction of the metal valence d orbitals due to the increased positive charge on the metal centers induced by the more electronegative substituent.

The $\text{XC}\div\text{MX}_3$ complexes have expectation values $\langle s^2 \rangle$ in the 2.007 to 2.010 range, which are in excellent agreement with the 2.000 value expected for a pure triplet state with two unpaired electrons.^{13,16} These triplet complexes contain a σ_z C–M single bond, and the two unpaired electrons in C_{px} and C_{py} orbitals are shared with metal d orbitals to form degenerate electron-deficient π bonds.¹³ Notice the increasing spin density on carbon and decreasing spin density on the metal center for both fluoride and chloride species as the metal size increases. The $\text{C}(2p)$ overlap with $\text{M}(nd)$ clearly decreases with increasing metal size. This decrease in $\text{C}\div\text{M}$ π bonding accompanies a decrease in halogen–carbon conjugation. The lowest spin on carbon for $\text{ClC}\div\text{TiCl}_3$ goes hand in hand with the shortest C–Ti bond, which has slightly more π -bonding character than the $\text{FC}\div\text{TiF}_3$ analogue. The corresponding chlorofluorocarbon complexes also show shorter C–M bonds for more α -Cl substituents.

The computed parameters for the triplet mixed halogen complexes are listed in Table S4 (Supporting Information). Here, the $\text{C}\div\text{M}$ bond length is shorter and stronger when two chlorine atoms (rather than two fluorine atoms) are attached to the transition metal center, which is in line with this effect for the pure halogen species. Again the Mulliken charge on the terminal halogen attached to the carbon switches charge sign when changed from fluorine to chlorine, whereas all halogens attached to the metal center remain negatively charged. Notice that the $\text{FC}\div\text{MFCl}_2$ complexes, which are the major product formed on deposition, are roughly 10 kcal/mol higher in energy than the corresponding $\text{ClC}\div\text{MF}_2\text{Cl}$ species. The latter increase at the expense of the former complexes on UV irradiation. This suggests that α -Cl transfer may be faster during reaction in the condensing sample, but the more stable α -F transfer product dominates after long-term exposure of the solid matrix sample to UV light.

Conclusions

Laser-ablated Ti, Zr, and Hf atoms react with CF_4 to form very stable low-energy triplet $\text{FC}\div\text{MF}_3$ complexes. These species possess strong C–F bonds, characterized by very high

C–F stretching frequencies, and a unique $C\equiv M$ electron-deficient triple bond. Reactions with CCl_4 formed the analogous $ClC\equiv MCl_3$ complexes, which have an even shorter computed $C\equiv M$ bond length, owing to less inductive contraction of the metal valence d orbitals. Reactions with CF_2Cl_2 formed both $FC\equiv MFCl_2$ and $ClC\equiv MF_2Cl$ complexes. The latter are lower in energy and increase at the expense of the former complexes on UV irradiation. The transfer of spin density from carbon to metal verifies the π -bonding interaction, which is favored by α -Cl over α -F substitution.

Acknowledgment is made to the Donors of the American Chemical Society Petroleum Research Fund for support of this research.

Supporting Information Available: Figures S1 and S2 for Zr, Hf, and CF_2Cl_2 infrared spectra and Tables S1, S2, S3, and S4 for calculated frequencies and structural parameters. This material is available free of charge via the Internet at <http://pubs.acs.org>.

OM070120G